Morphometric Analysis of Mesh Asymmetry

Václav Krajíček[1,2] Ján Dupej[1] Jana Velemínská[2] Josef Pelikán[1]
vajicek@cgg.mff.cuni.cz jdupej@cgg.mff.cuni.cz velemins@natur.cuni.cz pepca@cgg.mff.cuni.cz

[1] Department of Software and Computer Science Education, Charles University in Prague, Malostranské náměstí 25, 11800, Prague, Czech Republic

[2] Department of Anthropology and Human Genetics, Faculty of Sciences, Charles University in Prague, Viničná 7, 12844, Prague, Czech Republic

ABSTRACT

New techniques of capturing shape geometry for the purpose of studying asymmetry in biological objects bring the need to develop new methods of analyzing such data. In this paper we propose a method of mesh asymmetry analysis and decomposition intended for use in geometric morphometry. In geometric morphometry the individual bilateral asymmetry is captured by aligning a specimen with its mirror image and analyzing the difference. This involves the construction of a dense correspondence mapping between the meshes. We tested our algorithm on real data consisting of a sample of 102 human faces as well as on artificially altered meshes to successfully prove its validity. The resulting algorithm is an important methodological improvement which has a potential to be widely used in a wide variety of morphological studies.

Keywords

mesh asymmetry, geometric morphometry, mesh correspondence

1. INTRODUCTION

The geometry of an object reflects many facts about its creation development and purpose. A significant property observed in many biological objects is symmetry. Specifically, bilateral symmetry can be defined as the existence of a plane that splits an object into two identical parts with respect to reflection. This kind of symmetry is exhibited by most living natural objects (see Figure 1). Deviation from bilateral symmetry, asymmetry, can result from various stresses in population or individual development. Evaluation of asymmetry in the human face is useful in various scientific fields like anthropology, plastic surgery, forensic medicine, orthodintics, surgery, anatomy and others. Notably, the quantitative analysis of asymmetry provides important information for treatment planning; e.g. it can be used to determine the target area or the surgical method to be applied [Dam11].

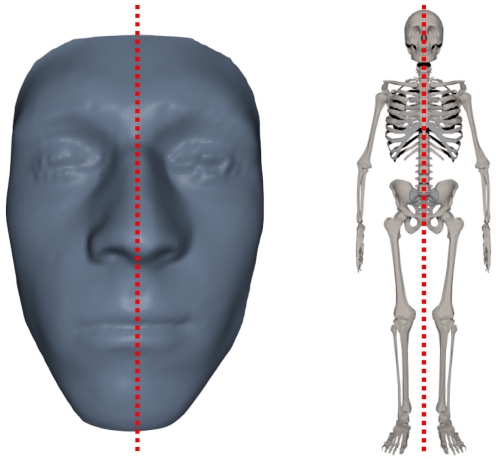

Figure 1: Examples of bilateral symmetry. It can be easily found in many higher and lower species.

Traditional and geometric morphometry, the tool of many fields of natural science such as botany, zoology or anthropology, offers ways to analyze the asymmetry of simple morphometric data such as lengths and landmark locations. However, with the advent of new measuring techniques such as surface and CT scanners to these fields new methods are required to analyze the full measure of information provided by these new data modalities.

Particularly we aim to develop an algorithm to analyze the asymmetry in triangular meshes in a way that is needed for geometric morphometry [Boo97],

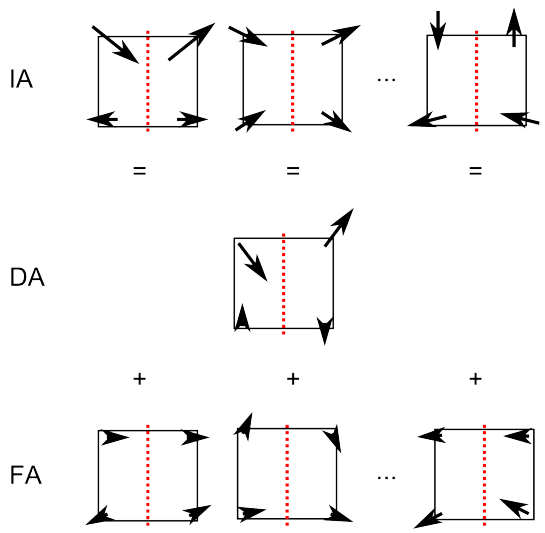

Figure 2: Decomposition of individual asymmetry (IA) into directional (DA) and fluctuating (FA) asymmetry components.

which includes its decomposition into directional and fluctuating asymmetry [Val62] [Pal94] [Kli02]. Before we analyze the group tendency to asymmetry we have to formulate how to interpret individual asymmetry.

Individual asymmetry is the quantified difference in a particular feature from its paired counterpart. Directional asymmetry is then the average of these differences across the studied sample. The statistical significance of this average can be evaluated using standard statistical tools such as the t-test. In other words, directional asymmetry describes the tendency to a certain deviation from the symmetry of the whole group or population. On the other hand, fluctuating asymmetry is defined as the difference between individual asymmetry and directional asymmetry and thus represents the random presence of asymmetry in the individual. Fluctuating asymmetry traits are normally distributed around the mid-sagittal plane. The overall magnitude of the fluctuating asymmetry is generally more significant than its spatial distribution. The process of such decomposition is visualized in the Figure 2.

In geometric morphometry, asymmetry is evaluated on paired features, i.e. paired landmarks and distances. The correspondence of particular features in traditional and geometric morphometry across the sample is known by definition from the homology of the features. Such correspondence is, however, not implicitly defined on triangular mesh data.

In the following chapter, some existing work related to mesh asymmetry analysis and extraction will be introduced. In Chapter 3 we will present the basis of our approach, namely the dense correspondence algorithm introduced by Hutton [Hut01]. Next, in Chapter 4 we thoroughly explain our procedure. We then we demonstrate its results in three scenarios in Chapter 5. Finally, Chapter 6 concludes our work and discusses future extensions.

2. RELATED WORK

Symmetry and asymmetry is an important feature of the human brain which was intensively studied in the past. In the modern era there have been many attempts [Fou11] to analyze MRI images and interpret brain asymmetry with respect to its connection to illnesses, functional abilities or genetics.

There have not been many attempts at automatic analysis of asymmetries in mesh data. One particular approach [Liu03] maps objects of interest onto a surrounding cylindrical surface. In the reference cylindrical coordinate system, the corresponding symmetric points are found with the help of manually placed landmarks. Asymmetry is then deduced from these pairs. This approach obviously works only for simple shapes that can be unambiguously projected onto a cylinder.

A different method [Ola07] assumes the existence of an ideally symmetric template and then maps each subject in the study onto this template using B-spline based non-rigid registration. Construction of the ideal or any symmetric template for a certain group is not trivial. Constructing that template requires the so called mid-sagittal plane about which the template is bilaterally symmetrical.

Another approach [Com08b] constructs a mid-sagittal plane using a modified EM algorithm [Com08a] and uses it to mirror the studied shapes. Asymmetry is then represented as the distance between the corresponding points on the original and mirror shape. Correspondence is found using non-rigid registration, bending the mirror shape to the original.

In geometric morphometry [Boo97], asymmetry was analyzed on landmark datasets [Sch06] by mirroring the landmark configuration and reordering the landmarks so that the mirror and the original can be realigned. The asymmetry is then defined as the difference of an ideally superimposed mirror and the original. More importantly, the approach decomposes the asymmetry in the traditional way studied in biological sciences [Val62] [Pal94].

We used some of these ideas in our proposed method.

3. DENSE CORRESPONDENCE

The individual asymmetry can be computed from the knowledge of matching counterpart features in a mirrored mesh. To calculate the directional and

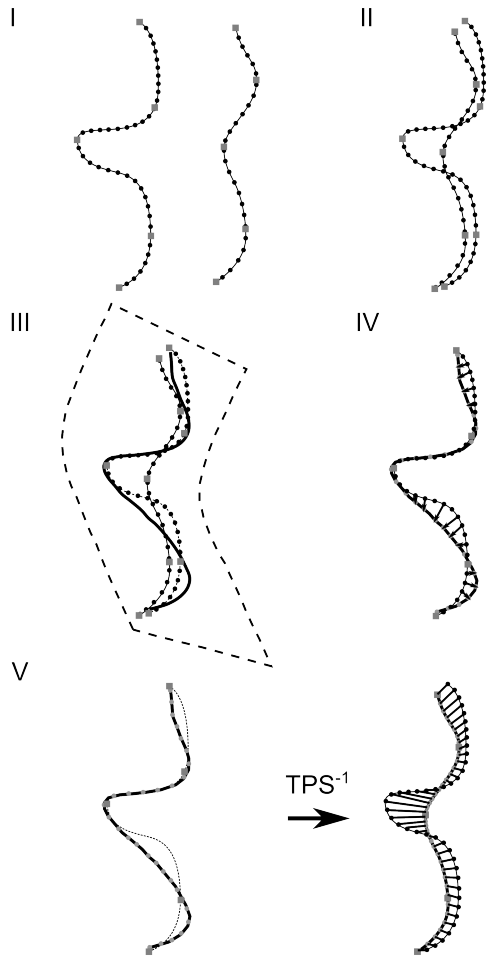

Figure 3: The steps of dense mesh correspondence construction in 2D. I-II) rigid alignment of input data, III) TPS deformation of the moving mesh, IV) nearest neighbor correspondence search, V) inverse TPS deformation of found points

fluctuating asymmetry, the matching of corresponding features in the group must be known.

Finding these matches equates to the construction of correspondence mapping either between a mesh and its mirror image of any two meshes in the group. Generally, any non-rigid mesh registration algorithm could be used for this task.

In the case of biological data we are also able to exploit homology – a unique one-to-one correspondence of certain features of interest. We therefore employ the following mesh correspondence construction.

The dense correspondence construction algorithm by [Hut01] [Hut03] uses sparsely landmarked surfaces. The more landmarks are used, the better the results. If possible, landmarks should be spread evenly over the area of interest. Placing all landmarks in one plane should be avoided as it will reduce the quality of correspondence. This is due to the fact that the spatial deformation describing the correspondences would

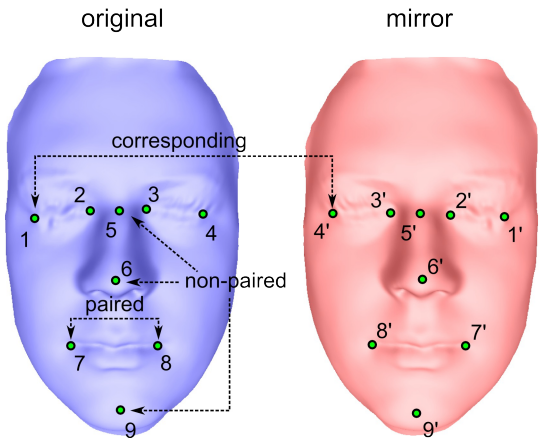

Figure 4: Original and mirror mesh.

not be defined well outside this plane. The mesh against which the correspondences are sought is designated the reference mesh, while the others are referred to as the moving meshes.

First, we rigidly align the moving mesh to the reference mesh by minimizing the squared distance of their respective landmarks using ordinary Procrustes superimposition, a method of rigid registration [Boo97] while preserving unit centroid size.

Second, the aligned moving mesh is bent to fit the reference mesh using thin-plate splines (TPS) interpolation

$$TPS(\vec{x}) = \vec{a}_0 + \vec{a}_1 x + \vec{a}_2 y + \vec{a}_3 z + \sum_{i=0}^{n} \vec{w}_i \varphi(\|\vec{x} - \vec{p}_i\|)$$

where $\vec{p}_i$ are landmark locations on the reference and φ is the radial basis function $\varphi(r) = r^3$. The TPS is fitted to the superimposed landmark pairs from the previous step. This way the meshes are brought as close as possible to each other so that the correspondences can be constructed.

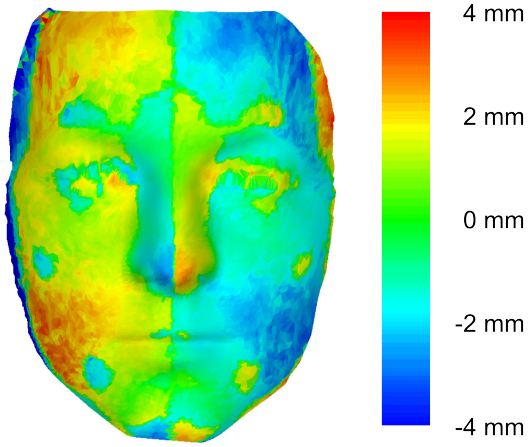

Figure 5: Symmetric face and individual asymmetry captured by the algorithm

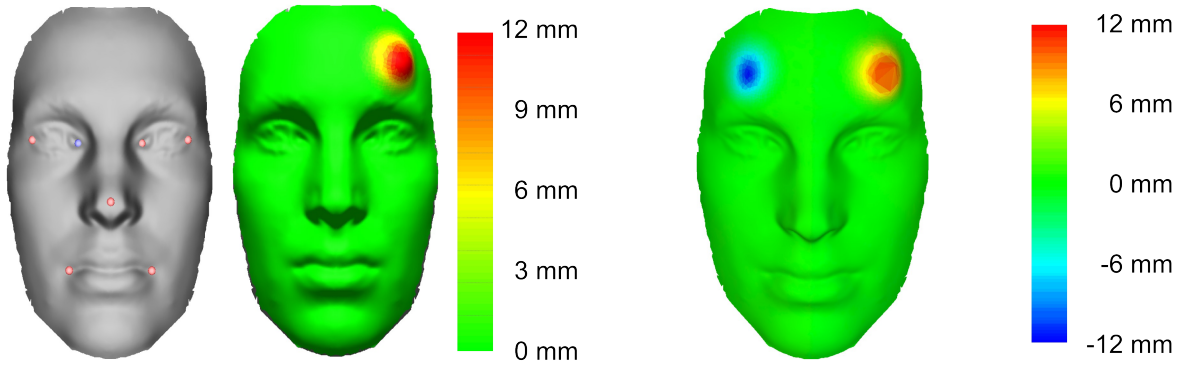

Figure 6: An ideally symmetric face and the artificially added asymmetry (left). Individual asymmetry of artificial test subject detected by the algorithm (right).

In the last step the reference mesh is used to construct a new mesh with the same topology as the reference but the shape of the moving mesh, which is referred to as the correspondence mesh. This is done by finding the closest point (not necessarily vertex) in the reference mesh to each vertex of the moving mesh. The search efficiency can be enhanced with acceleration structures. A kd-tree on all mesh triangles has proven very effective. This process yields the correspondence between the reference mesh's points and the deformed moving mesh. We now need to transform these vertex locations to the space of the original moving mesh. Because the deformed mesh was created with a TPS the original is obtained by inverting that TPS. Since TPS has no analytically defined inversion it must be computed numerically as the solution of the following minimization problem.

$$\underset{\vec{x}\in R^3}{\boldsymbol{arg\ min}} \|TPS(\vec{x})-\vec{y}\|^2$$

This could be solved by any optimization procedure. Because in this case the second derivatives can be easily analytically expressed, the Newton's method is suitable for the problem.

An alternative to the numeric TPS inversion computation is an approximation using barycentric coordinates. The correspondence points in the deformed moving mesh are expressed in barycentric coordinates inside their respective triangles. The same barycentric coordinates are then used to compute the point in the corresponding face of the original moving mesh. A scheme of the correspondence construction procedure is described in Figure 3.

Sometimes the corresponding point is located too far from the vertex in the reference. Then it is not likely that it is a proper correspondence. We can define a threshold distance beyond which the correspondence is not accepted. In that case we simply omit this vertex from the mesh with identical topology.

In order to analyze a group of meshes the correspondences across the whole sample must be constructed. One mesh from the sample is chosen as the reference and the remaining meshes are used as moving meshes to construct correspondences to the reference.

The choice of the reference mesh may have a significant influence on the result. It should be chosen so that it is not too different from the rest of the group. Ideally, it lies in the middle of the group, hence the other moving shapes need to be bent less to align with the reference. The authors of the original algorithm [Hut01] claim that if the input data is random, choosing the first mesh as the reference for the group is as good as choosing any other.

4. MESH ASYMMETRY ANALYSIS

In our approach to capture a group mesh asymmetry we use the concept of decomposing the asymmetry into directional and fluctuating components. Concurrently, dense triangular meshes allow us to express the asymmetry on a very localized level.

Before we can compare the local asymmetries in all meshes, we need to have them transformed into a common coordinate space. This is done by applying a group-wise rigid landmark-based registration, specifically generalized Procrustes superimposition has been used. The meshes' vertices are transformed the same way as the landmarks in the Procrustes superimposition.

The next step is to recompute the meshes to the same number of vertices and the same topology. We used the dense correspondence construction algorithm from the previous section.

Now, the individual mesh asymmetry is computed. The result is the list of directions for every vertex. If every vertex were moved by their respective displacement the mesh would become ideally symmetric. The mirror mesh must be constructed by

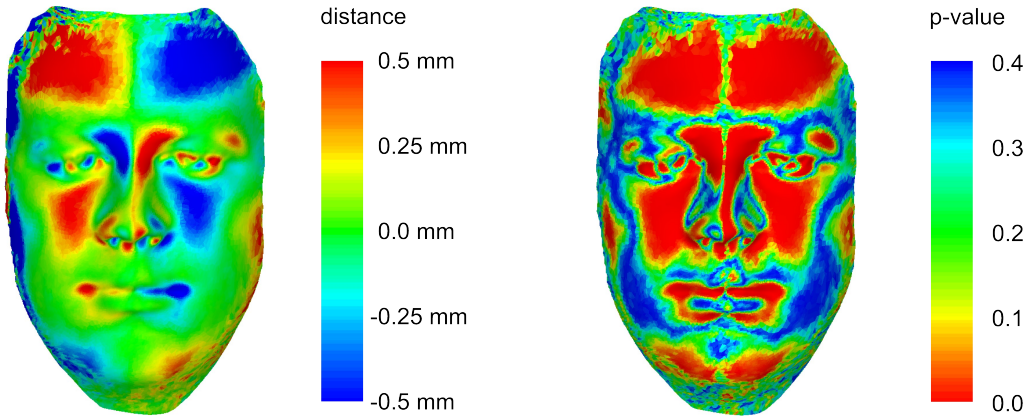

Figure 7: Directional asymmetry (left) and significance map of the asymmetry (right) on 102 human faces.

negating one of the vertex coordinates (see Figure 4). The same is done with landmarks placed on the mesh.

The landmarks are then used to align the mirror mesh back to the original mesh. In order to do that the landmarks must be reordered as they have changed their homologous meaning after the mirroring. e.g. some landmarks on the left side of a bilaterally symmetric mesh became the landmarks on the right side of the mirror mesh. These are the so called paired landmarks; they swap their positions with their mirror counterparts, while the others, the non-paired landmarks are not affected by mirroring.

After mirroring and landmark reordering the mirror meshes are realigned by ordinary Procrustes superimposition and deformed by TPS in order to get mirror meshes closer to the original ones and allow for subsequent correspondence searching. The closest points on the mirror meshes to each vertex of the original correspondence meshes are found using search acceleration structures. Again, we opted for a kd-tree.

The vectors defined by the difference of the original mesh vertices and their closest mirror mesh points is the local measures of asymmetry. Completely symmetrical shapes have identical mirrors and when aligned the distances between the original mesh vertices and the closest points are zero. If asymmetries occur on the mesh the difference between the left and right part of the mesh appears and the distance between a part of the mesh and its mirrored counterpart becomes non-zero. Furthermore, the associated vector holds the information about the direction of the asymmetry, i.e. how the part of the mesh was moved to form the asymmetry. This information is exhibited on either side of a bilaterally symmetrical mesh in the opposite directions. Hence it cannot be said which part of the mesh originated from a symmetric shape and which was altered, if this is the way the analyzed asymmetric shape was created. It can be said that bilateral asymmetry is a symmetric feature. The vector field that represents the displacement of a point on a mesh from where it would lie if the mesh were ideally symmetric is called individual asymmetry.

We visualize the aforementioned vector field on the original mesh with color-coded signed distances (see Figure 5). The sign is the same as that of the dot product of the mesh normal and the vector of individual asymmetry in that point. The color images could be simply interpreted in the following way: red areas lie in the front of the corresponding mirrored counterpart which means that they are larger than the corresponding paired counterpart while blue areas are smaller and lie behind the aligned mirrored counterpart. The areas that are close to green are not significantly larger or smaller. This interpretation does not include any information about the direction

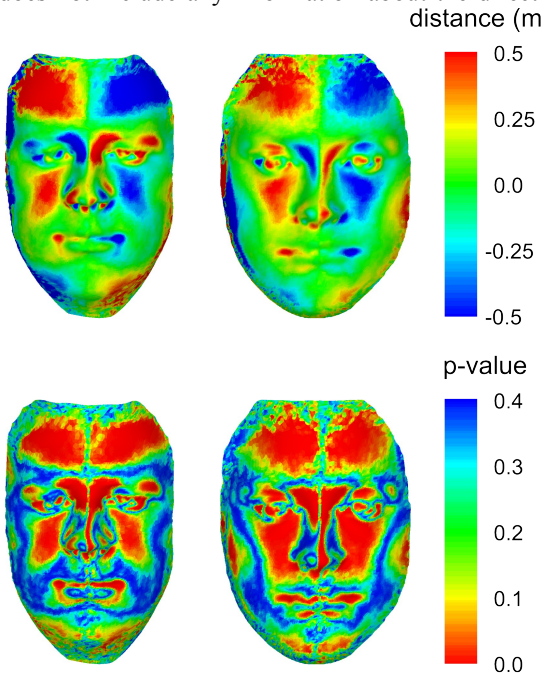

Figure 8: Directional asymmetry of male (left) and female (right) subgroups.

of the asymmetry. This sort of visualization is also known as clearance vector mapping and is useful in quantifying the facial surface asymmetries in the areas where anthropometric landmarks are scarce. The volume of detected asymmetry is potentially significant in patients who may have their unilateral facial deficiencies corrected using injections or implants [OGr99].

All individual asymmetries are already aligned group-wise, therefore, directional asymmetry is computed as the average of all corresponding individual asymmetry vectors. The length of the respective individual asymmetry vectors is the same for all the meshes and they correspond to each other per element as the meshes were reconstructed to have the same topology. The directional asymmetry is visualized the same way as individual asymmetry.

Fluctuating asymmetry is computed as the difference of individual asymmetry and directional asymmetry. Its visualization is also based on color coded distances without the consideration of the sign for direction as was done for individual and directional asymmetry above. As stated in the previous chapter, we are more interested in the overall magnitude of the fluctuating asymmetry which is computed as the sum of squared distances of the fluctuating asymmetry vectors. It can be compared across the group and if normalized by the number of vectors, or between groups just as well.

To prove that the directional asymmetry reflects the global trend of the group, and is not the result of randomness in the group, it has to be tested statistically. A standard t-test is performed on the signed lengths of corresponding individual asymmetry vectors. The significance map can then also be visualized. This way of interpretation is especially important for particular research in biological sciences.

The direction of the individual asymmetry vector is also important property that should be taken into account. In order to do so we define the local orientation difference asymmetry measure which is equal to cosine of angle between corresponding individual asymmetry vectors.

The lengths of individual asymmetry vectors and local orientation difference asymmetry measure can be summarized into total asymmetry and total orientation asymmetry.

$$TA = \frac{1}{N}\sum_{i=0}^{N} \left\| \vec{a}_i \right\|^2$$

$$TOA = \frac{1}{N}\sum_{i=0}^{N} \vec{n}_i \cdot \vec{m}_i$$

5. RESULTS

Our semiautomatic landmark-based approach reflects the needs of scientists from fields like archaeology and anthropology where the homology of certain feature points is advantageous. It is often the case that mesh datasets together with their respective landmark configurations already exist and the results of landmark-only based studies have already been published so some comparison of results can be done. All these facts are the motivation supporting our solution over completely autonomous algorithms, e.g. employing nonrigid mesh registration.

In the first test it will be demonstrated how the proposed algorithm approximates individual asymmetry on an artificial dataset where the ground truth is well known. A symmetric face model was created by cutting a real face in half approximately along its medial axis mirroring one of the halves and stitching it to its original. Then the symmetric face was locally deformed, bulged on the left side of the forehead. Shell distance measured by a software tool, RapidForm XOS in our case, was used as the ground truth (see the left side of Figure 6). In this case, if the deformation does not affect the areas with landmarks, the algorithm can uncover the asymmetry perfectly (see the right side of Figure 6). If the location of a landmark is distorted by a nearby asymmetry the error of alignment by the generalized Procrustes superimposition will be distributed among all

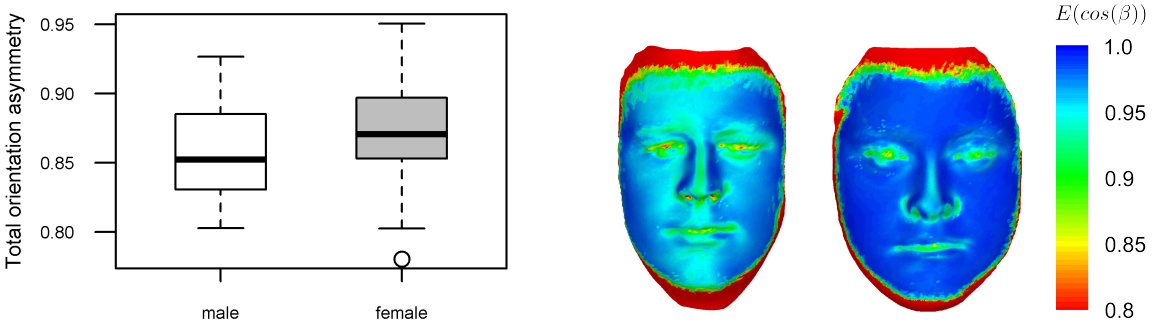

Figure 9: Difference in total orientation asymmetry of male and female subgroups is statistically significant ($p < 0.05$). The orientation the asymmetry is locally unevenly distributed on the male faces while being uniform almost everywhere on female faces.

landmarks. Even in this case the algorithm still reveals the asymmetry relatively well. In case of large asymmetries all across the mesh it would be difficult for any method to recover results close to ground truth as in this kind of problem it is highly ambiguous what the original symmetric shape is. Therefore in practice, landmarks are usually placed on stable locations. These locations may exhibit asymmetry as well, it is however assumed that the user will choose a landmark configuration whose own asymmetry will have the least impact on the results.

In the second test a group of 102 real faces were analyzed. The faces were captured by a *InSpeck 3D MegaCapturor II* scanner with 0.4 mm resolution in the direction of its optical axis. The resulting meshes with approximately 100k-200k triangles were cleaned and trimmed from border areas and finally decimated to approximately 20k-30k triangles. Our landmark configuration contains nine landmarks situated in the corners of mouth, eyes, and on the tip and around the nose. The landmarks were placed by an expert. The resulting directional asymmetry can be seen in the left side of Figure 7. The significance map of the asymmetry is in right side of Figure 7. The group includes both male and female subjects. Each sex can be analyzed separately and compared (see Figure 8). Local asymmetry information can be summarized into a single value per specimen called total asymmetry. Neither individual asymmetry nor total asymmetry discriminates between sexes in our sample. On the other hand, the total orientation asymmetry shows the difference rather clearly (see Figure 9). This finding is confirmed by results from [Liu03] which indicates that the orientation asymmetry is important in comparative studies. Our method is new in ability to capture asymmetry and correspondence in more complex shapes.

In the third (Figure 10) test we used 50 scans of human palate (a convex surface surrounded by dental arc). The shape of this particular structure is studied in order to describe impact of the therapy on patients with cleft of the lip and palate. Specifically the palate has an altered shape and its further development is influenced by inadequate growth of maxilla. The shape of the palate has great individual variation. The above-described methodology is useful for the comparison of the palatal shape depending on the type and extent of the cleft, the utilized surgical method and the surgeon's proficiency, as well as numerous other factors associated with surgical and orthodontic treatment [Sma03]. The shape of the palate is a problematic object from the view of geometric morphometry as the only apparent landmarks can be placed at the locations of teeth.

The whole algorithm is not very computationally demanding. The analysis of all 102 faces took approximately 283 seconds on Intel Core i7 machine. The computation consists of many independent parts that can be computed in parallel. For instance the group correspondence construction in fact involves N independent processes, N being the count of meshes in the group. Similarly, individual mesh asymmetry can be computed independently for each mesh.

6. CONCLUSIONS

The dense correspondence algorithm has been used in many geometric morphometry studies, e.g. [Ham04] [Bej12] [Vel12]. It extends the ability of GMM methodology to capture shapes from simple primitives such as homologous landmark to triangular meshes representing the whole surface of the object. We continued in this trend to study asymmetry of groups of shapes in a novel way but using the traditional approach of decomposition into directional and fluctuating asymmetry.

The most significant contribution of our work is the application of dense correspondence mapping, as introduced in [Hut01], to map asymmetries onto complex geometry, as opposed to [Liu03] that only used cylindrical surfaces. Furthermore, our approach utilizes landmark-based registration, which makes it more adjustable in certain scenarios than most automatic algorithms [Com08b].

From a practical point of view and in comparison to commercially available tools implementing dense correspondence modeling algorithms such as

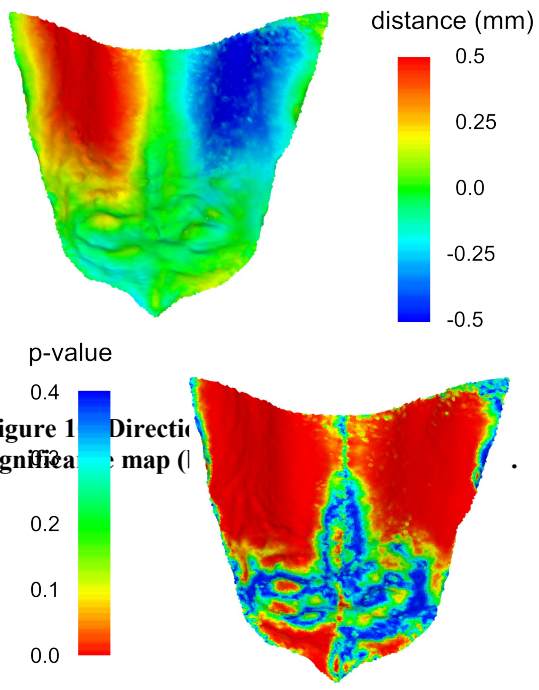

Figure 1 Directi… significa… map (l… .

MorphoStudio 3.0 (from BioModeling Solutions, 2006) we sped up the correspondence matching by employing a kd-tree search data structure.

7. ACKNOWLEDGEMENTS

Our thanks goes to the members of Laboratory of 3D Analytical and Visualization methods, Charles University in Prague for providing us with real data. This research has been supported by GAUK 309611 research grants from the Grant Agency of Charles University in Prague and MSM 0021620843 from the Ministry of Education, Youth and Sports of the Czech Republic.

8. REFERENCES

[Bej12] Bejdová, Š., Krajíček, V., Peterka, M., Trefný, P., and Velemínská, J. Variability in Palatal Shape and Size in Patients with Bilateral Complete Cleft Lip and Palate Assessed Using Dense Surface Model Construction and 3D Geometric Morphometrics, J Cranio Maxill Surg, 40 [3]:201–208, 2012.

[Boo97] Bookstein, F.L. Morphometric Tools for Landmark Data : Geometry and Biology, Cambridge University Press, 1997.

[Com08a] Combes, B., Hennessy, R., Waddington, J., Roberts, N., and Prima, S. Automatic Symmetry Plane Estimation of Bilateral Objects in Point Clouds, In IEEE Conference on Computer Vision and Pattern Recognition (CVPR'2008), Anchorage, USA, IEEE, 2008.

[Com08b] Combes, B. and Prima, S. New Algorithms to Map Asymmetries of 3D Surfaces, In Proceedings of the 11th International Conference on Medical Image Computing and Computer-Assisted Intervention - Part I, Berlin, Heidelberg, Springer-Verlag, pp.17–25, 2008.

[Dam11] Damstra, J., Oosterkamp, B.C.M., Jansma, J., and Ren, Y. Combined 3-dimensional and Mirror-image Analysis for the Diagnosis of Asymmetry, Am J Orthod Dentofac, 140 [6]:886–894, 2011.

[Fou11] Fournier, M., Combes, B., Roberts, N., Keller, S., Crow, T.J., Hopkins, W.D., and Prima, S. Surface-based Method to Evaluate Global Brain Shape Asymmetries in Human and Chimpanzee Brains, In Proceedings of the 8th IEEE International Symposium on Biomedical Imaging: From Nano to Macro, Chicago, USA, IEEE, pp.310–316, 2011.

[Ham04] Hammond, P., Hutton, T.J., Allanson, J.E., Campbell, L.E., Hennekam, R.C.M., Holden, S., Patton, M.A., et al. 3D Analysis of Facial Morphology, Am J Med Genet, 126A [4]:339–348, 2004.

[Hut01] Hutton, T.J., Buxton, B.F., and Hammond, P. Dense Surface Point Distribution Models of the Human Face, In Proceedings IEEE Workshop on Mathematical Methods in Biomedical Image Analysis, Kauai, Hawaii, IEEE, pp.153–160, 2001.

[Hut03] Hutton, T.J., Buxton, B.F., Hammond, P., and Potts, H.W.W. Estimating Average Growth Trajectories in Shape-space Using Kernel Smoothing, IEEE Trans Med Imaging, 22 [6]:747–753, 2003.

[Kli02] Klingenberg, C.P., Barluenga, M., and Meyer, A. Shape Analysis of Symmetric Structures: Quantifying Variation Among Individuals and Asymmetry, Evolution, 56 [10]:1909–1920, 2002.

[Liu03] Liu, Y. and Palmer, J. A Quantified Study of Facial Asymmetry in 3D Faces, In Proceedings of the IEEE International Workshop on Analysis and Modeling of Faces and Gestures, Nice, France, IEEE, pp.222–229, 2003.

[OGr99] O'Grady, K.F. and Antonyshyn, O.M. Facial Asymmetry: Three-Dimensional Analysis Using Laser Surface Scanning, Plast Reconstr Surg, 104 [4]:928–937, 1999.

[Ola07] Ólafsdóttir, H., Lanche, S., Darvann, T.A., Hermann, N.V., Larsen, R., Ersbøll, B.K., Oubel, E., et al. A Point-wise Quantification of Asymmetry Using Deformation Fields: Application to the Study of the Crouzon Mouse Model, In Proceedings of the 10th International Conference on Medical Image Computing and Computer-assisted Intervention, Berlin, Heidelberg, Springer-Verlag, pp.452–459, 2007.

[Pal94] Palmer, A.R. Fluctuating Asymmetry Analyses: A Primer, In Proceedings of the International Conference on Developmental Instability: Its Origins and Evolutionary Implications, Dordrecht, The Netherlands, Kluwer, pp.335–364, 1994.

[Sch06] Schaefer, K., Lauc, T., Mitteroecker, P., Gunz, P., and Bookstein, F.L. Dental Arch Asymmetry in an Isolated Adriatic Community, Am J Phys Anthropol, 129(1):132–42, 2006.

[Sma03] Šmahel, Z., Trefný, P., Formánek, P., Müllerová, Ž., and Peterka, M. Three-Dimensional Morphology of the Palate in Subjects With Isolated Cleft Palate at the Stage of Permanent Dentition, Cleft Palate-Cran J, 40 [6]:577–584, 2003.

[Val62] Van Valen, L. A Study of Fluctuating Asymmetry, Evolution, 16 [2]:125–142, 1962.

[Vel12] Velemínská, J., Bigoni, L., Krajíček, V., Borský, J., Šmahelová, D., Cagáňová, V., and Peterka, M. Surface Facial Modelling and Allometry in Relation to Sexual Dimorphism, Homo, 63 [2]:81–93, 2012.